

Compression Creep of Molten Low-Density Polyethylene

J. V. ALEMAN

Instituto de Ciencia y Tecnologia de Polimeros, Juan de la Cierva 3, 28006 Madrid, Spain

SYNOPSIS

Viscoelastic parameters of low-density polyethylene melt (LDPE) in compression creep have been measured. Volume deformation ($k\%$) increases as pressure (P) increases and temperature (T) decreases. Plots of the bulk creep compliance $B(t)$ vs. time (t) may be shifted to provide master curves. As the pressure and the temperature increase, the pressure shift factors (b_p and a_p) increase almost linearly [activation volumes (ΔV^*) varying from 1.0 to 15.0 cm³ mol], while the temperature-shift factors (b_T and a_T) decrease. The steady-state creep compliance (B^s) describes the recoverable storage of elastic energy (Be) and seems to be related to the extrusion die-swell (B_c^s/B_d^s). Volume viscosity (η_K) decreases with increasing stress (P) and increasing temperature (T).

INTRODUCTION

Melt compression creep has been described so far only for rigid* polymers such as poly(butylene terephthalate) (PBT)⁴ (planar chains with aromatic rings and $-\Delta F^{600K} = 458$ J/g) and polystyrene (PS)⁵ (helical chains with side groups and $-\Delta F^{450K} = 500$ J/g).

To further explain the effect of chain structure on the creep behavior, polymers with flexible* chains ($-\Delta F^{450K} \approx 200$ – 250 J/g) and linear chains [poly(ethylene oxide) [PEO], helical, polar],² as well as long branches (low-density polyethylene [LDPE], planar, nonpolar)³ are being studied. This paper deals with the compression creep behavior of molten LDPE. Its equilibrium compression properties (P - V - T) have been described elsewhere.⁶⁻⁹

EXPERIMENTAL

Materials

LDPE P-033 was provided without additives by Repsol Quimica SA (Spain). Its molecular charac-

teristics have been described elsewhere.³ A silicone lubricant-type Rhodosil 47-V-300 from Siliconas Hispanicas SA (Spain) was used to avoid friction at the walls.

Methods

All compression measurements were carried out in an Instron capillary rheometer attached to an Instron tensile tester model TT-CM, with a steel plug instead of the capillary.¹⁰

The rheometer barrel (area $A = 0.907$ cm²) was preheated to the temperature of 337 K. Dial reading provided the zero setting (l^0). Afterward, 4.5000 g of LDPE pellets was added, and a Rulon plug of length l_r was introduced in the cylinder. A vacuum of 0.2 mmHg was then applied for 15 minutes for the polymer pellets to melt without bubbles. The barrel was then heated to the run temperatures of 423–463 K. The equilibrium in force (F) and temperature (T) was attained under a load of 1 kg, and to operate without degradation, the vacuum was replaced by an atmosphere of 99.9992% pure nitrogen. Since the experimental temperatures were all well above the polymer glass transition temperature ($T_g = 183$ K), the thermodynamic equilibrium was established rapidly, and, consequently, the initial volume of polymer (V_0) is a function of temperature only.

The machine crosshead was lowered at selected rates (usually 2 cm/min for the 5 and 30 MPa runs,

* Polymer melt chain rigidity has been assumed to be¹⁻³ the Gibbs free energy ($-\Delta F$), composed of intramolecular interactions (enthalpy, ΔH) and interchain interactions (entropy, $T \cdot \Delta S$), computable by graphical integration of specific heat (C_p) vs. temperature curves.

5 cm/min for the 70 and 100 MPa ones, and 10 cm/min for the 130 and 170 MPa runs) in order to achieve the pressure ($P = F/A$) chosen for the experiment (from 5 to 170 MPa), which was then kept constant while the changes in length (Δl_c) with time (t) were recorded. Actual results are shown in Figure 1 at 423 K and 100 MPa as a representative example.

The initial length (l_i) was computed from the crosshead speed, the paper speed (20 cm/min), and the paper length (l_p cm) between the points where the force started to increase and reached the constant value selected (at which the dial reading after 10 s was $l_{10''}$), respectively,

$$l_i = 0.25 \times l_p + l_{10''} \quad (1)$$

The actual initial length of the polymer (l_0) is

$$l_0 = l_i + l_s - l_r \quad (2)$$

in which l_s (1.25 cm) is the plunger travel security length.

Thus, it was possible to know the initial volume of the polymer:

$$V_0 = V_{0.1,T,0} = \pi R^2(l_0 - l^0) \quad (3)$$

The length of the polymer at any time (l_c) was then computed:

$$l_c = \Delta l_c + l_s - l_r + (\Delta l_r + \Delta l_{app})_c \quad (4)$$

in which Δl_r is the change with pressure of the Rulon plug length and Δl_{app} is the compliance (background response) of the experimental equipment.⁵

The volume V_c at $t = t_c$ is therefore

$$V_c = V_{P,T,t} = \pi R^2(l_c - l^0) \quad (5)$$

Dial reading was continued until a steady-state volume was attained. Then, the polymer decompression was started by reducing the pressure of the system to a constant value of 1 or 2 MPa according to the run being carried out. The increase in length of the polymer (Δl_d) with time was registered.

The length of the polymer (l_d) at $t = t_d$ is now

$$l_d = \Delta l_d + l_s - l_r + (\Delta l_r + \Delta l_{app})_d \quad (6)$$

The decompression volume is

$$V_d = \pi R^2(l_d - l^0) \quad (7)$$

The change in volume of the sample is

$$\Delta V_c = V_0 - V_c \quad (8a)$$

$$\Delta V_d = V_c - V_d \quad (8b)$$

The experimental procedure was tested with poly(ethylene terephthalate).^{4,11}

RESULTS AND DISCUSSION

V values at temperatures 423, 433, 443, 453, and 463 K and pressures 5, 30, 70, 100, 130, and 170 MPa

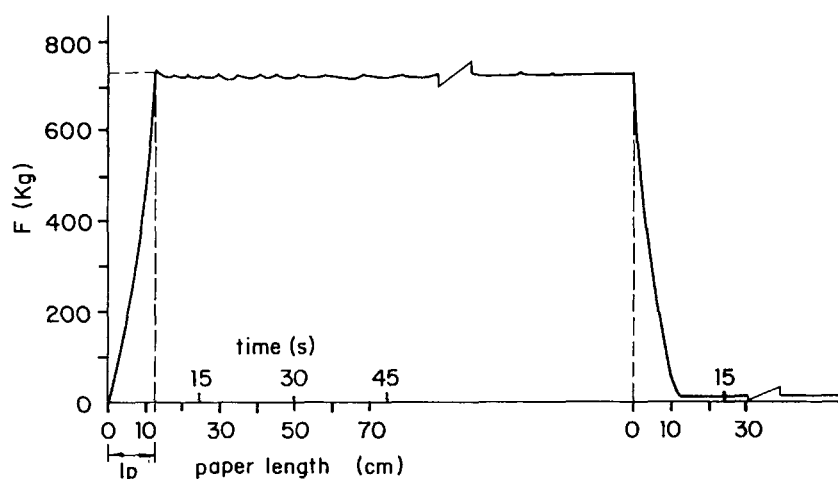


Figure 1 LDPE force (F) vs. time (paper length l_p) at 423 K and 100 MPa.

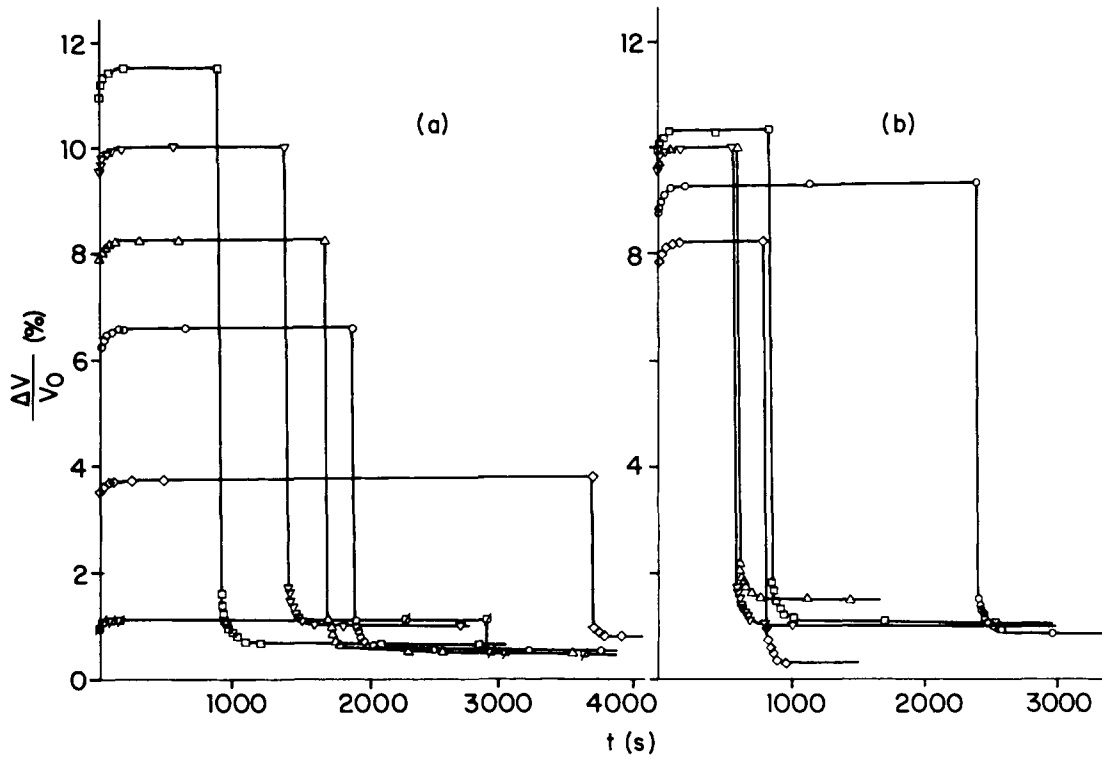


Figure 2 LDPE volume deformation ($k\%$) vs. time (t) as a function of (a) pressure at 453 K: (\square) 5 MPa, (\diamond) 30 MPa, (\circ) 70 MPa; (\triangle) 100 MPa, (∇) 130 MPa, (\square) 170 MPa; (b) temperature at 130 MPa: (\diamond) 423 K, (\circ) 433 K, (\triangle) 443 K, (∇) 453 K, (\square) 463 K.

were used to compute the volume deformations ($k\%$):

$$k_c\% = \frac{\Delta V_c}{V_0} \cdot 100 \quad (9a)$$

$$k_d\% = \frac{\Delta V_d}{V_0} \cdot 100 \quad (9b)$$

These are plotted vs. time (t) in Figure 2(a) and (b) at 453 K and 130 MPa, respectively, as representative examples. As may be observed, the volume deformation ($k\%$) is larger the higher the pressure and the lower the temperature. LDPE time-dependent volume (Fig. 3; the retardation times depend on temperature, pressure, and instantaneous state [$\Delta V/V_0$] of the polymer)¹² extends over 2 decades of logarithmic times.

The bulk compression creep compliance $B(t)$ may be computed from Figure 2 data as

$$B(t) = \frac{k(t)}{P} \quad (10)$$

A plot of $B(t)$ vs. t is shown in Figure 4(a) and (b) as a function of pressure and temperature, respectively. They can be reduced to a master curve by shifting them along the coordinate axis (Figs. 5 and 6).

Pressure-shift factors b_p^\dagger and a_p^\dagger were computed as^{12,13} (at equilibrium, LDPE compression follows Tait's equation)^{6,9}

[†] Bulk creep compliance $B(t)$ is the reciprocal of the bulk compression modulus of elasticity ($L = P/(\Delta V/V_0)$).² When L is plotted vs. the intramolecular interactions (ΔH) at 450 K, a straight line results that obeys the equation (with $L_0 \approx 4000$ MPa and $\alpha \approx 2.5$ MPa/(J/g))²:

$$L = L_0 - \alpha \cdot \Delta H^{450K} \quad (11a)$$

Consequently, the following equations are obtained:

$$b_p = \frac{L(P)}{L(P_0)} = \frac{L_0 - \alpha \cdot (\Delta H)_P}{L_0 - \alpha \cdot (\Delta H)_{P_0}} \quad (11b)$$

$$b_T = \frac{L(T_0)}{L(T)} = \frac{L_0 - \alpha \cdot (\Delta H)_{T_0}}{L_0 - \alpha \cdot (\Delta H)_T} \quad (13a)$$

Results according to them are plotted in Figures 7 and 8 (dashed lines).

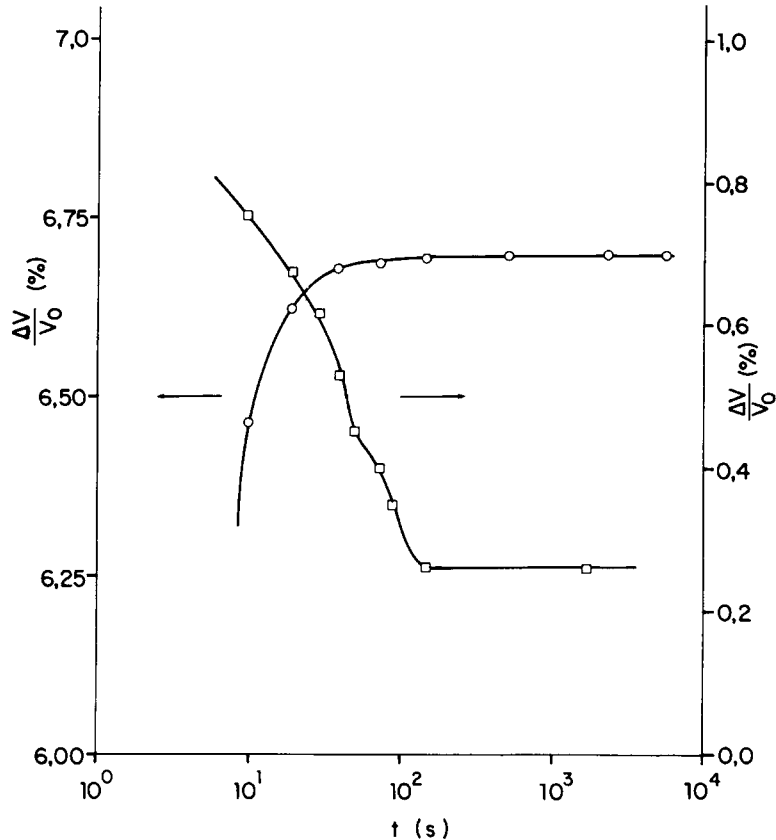


Figure 3 LDPE volume deformation ($k\%$) vs. time (t) at 423 K and 100 MPa: (○) compression, (□) decompression.

$$b_p = \frac{B(t, P_0)}{B(t, P)} \quad (11)$$

$$a_p = \frac{(\ln t)_{P_0}}{(\ln t)_P} \quad (12)$$

Figure 7 shows that b_p as well as a_p increase almost linearly as the compression stresses (P) and temperatures (T) increase.

Temperature-shift factors b_T and a_T computed as^{12,13}

$$b_T = \frac{B(t, T)}{B(t, T_0)} \quad (13)$$

$$a_T = \frac{(\ln t)_T}{(\ln t)_{T_0}} \quad (14)$$

[†] a_p has been described in the glassy state by eq. (12):

$$a_p = \exp\left(\frac{\Delta V^*}{R \cdot T_0} \cdot P\right) \quad (12a)$$

A plot of $\ln a_p$ vs. P should provide straight lines [Fig. 7(b)]. ΔV^* is the activation volume of the value of about 1–15 cm³/mol. The same scatter of data is always observed with flexible chain polymers,^{2,3} because their large volume changes make more noticeable the nonlinear response of the free volume. a_T obeys the equation

$$a_T = \exp\left[\frac{\Delta E}{R \cdot T_0^2} \cdot (T - T_0)\right] \quad (14a)$$

R is the gas constant and $\Delta E = 104$ KJ/mol³ is the LDPE compression flow activation energy. Results are shown in Figure 8(b) (dashed line).

decrease as the temperature and pressure (except at 5 MPa because the system is in the *gauche* conformation—see next paragraph) increase (Fig. 8).

Bulk creep compliance $B(t)$ behavior [Fig. 9(a) and (b)] is consequently different below and above some critical value of the process variables ($T_c \approx 443$ K and $P_c \approx 30$ MPa), which is presumed to be^{3,7,14} the *gauche-trans* transition. Below it, the compression of the free volume plus the occupied volume^{12,13} takes place. Above it, $B(t)$ may be con-

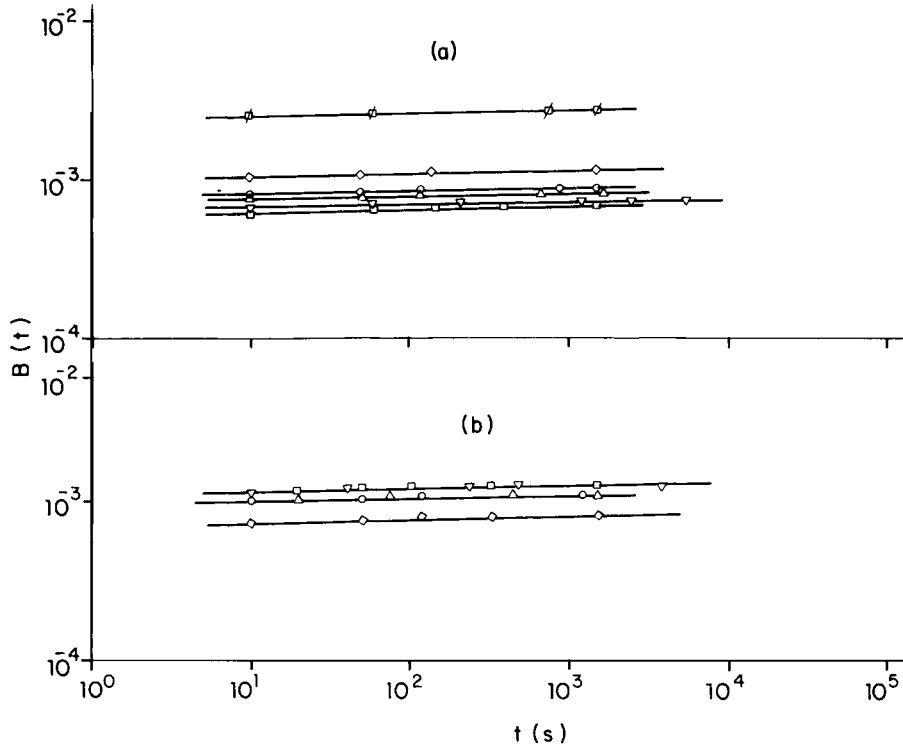


Figure 4 Bulk creep compliance $B(t)$ vs. time (t) at (a) 433 K and (\boxtimes) 5 MPa, (\diamond) 30 MPa, (\circ) 70 MPa, (\triangle) 100 MPa, (∇) 130 MPa, (\square) 170 MPa; (b) 30 MPa and (\diamond) 423 K, (\circ) 433 K, (\triangle) 443 K, (∇) 453 K, (\square) 463 K.

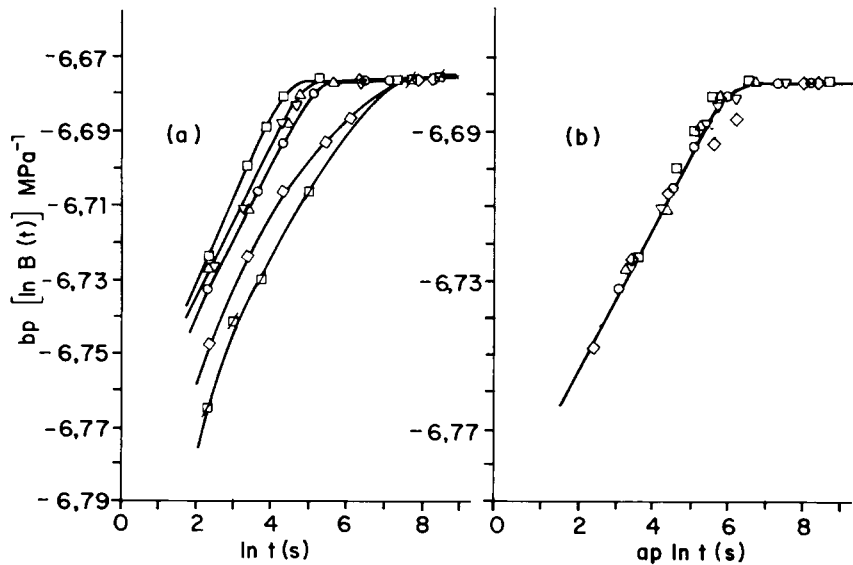


Figure 5 Bulk creep compliance $B(t)$ as a function of pressure at $T = 453$ K with reference pressure $P_0 = 30$ MPa: (\boxtimes) 5 MPa, (\diamond) 30 MPa, (\circ) 70 MPa, (\triangle) 100 MPa, (∇) 130 MPa, (\square) 170 MPa, shifted parallel to (a) the ordinate axis (b_p) and (b) the abscissa axis (a_p).

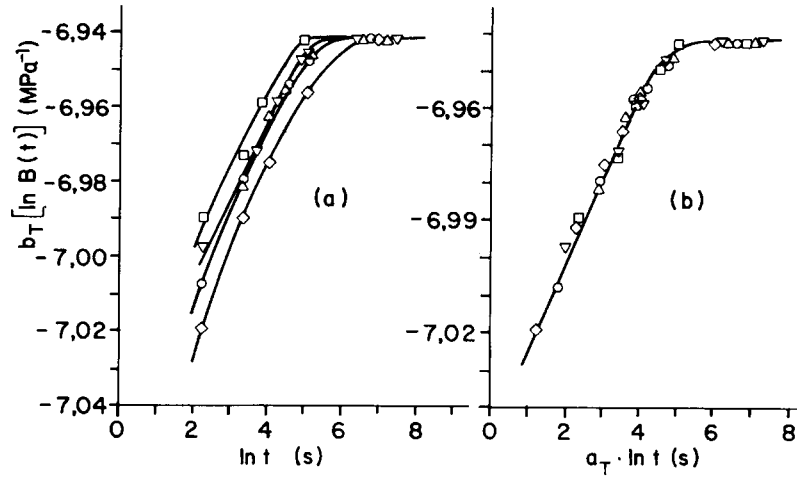


Figure 6 Bulk creep compliance $B(t)$ as a function of temperature at $P = 70$ MPa with reference temperature $T_0 = 463$ K: (\diamond) 423 K, (\circ) 433 K, (\triangle) 443 K, (∇) 453 K, (\square) 463 K, shifted parallel to (a) the ordinate axis (b_T) and (b) the abscissa axis (a_T).

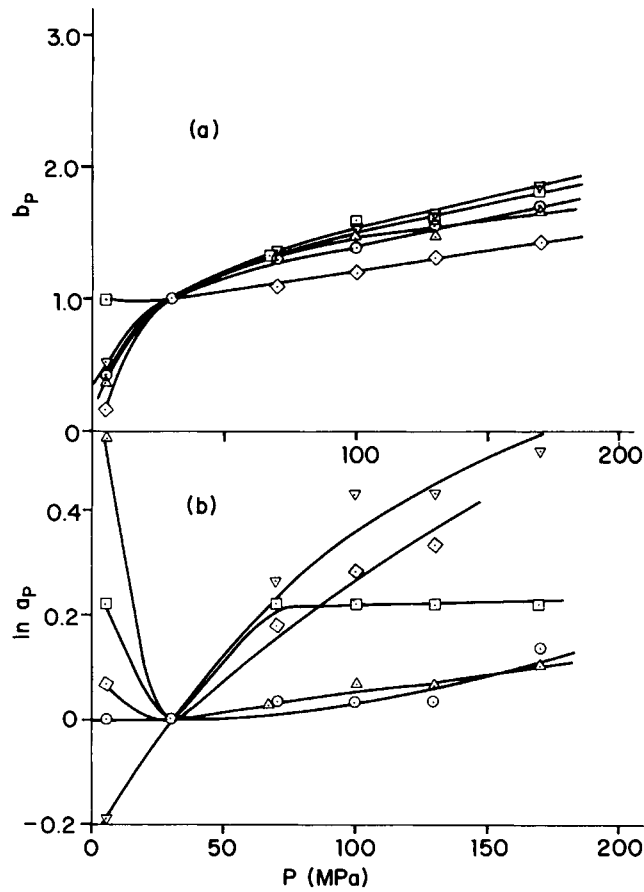


Figure 7 Pressure-shift factors with reference pressure $P_0 = 30$ MPa, at different temperatures (\diamond) 423 K, (\circ) 433 K, (\triangle) 443 K, (∇) 453 K, (\square) 463 K: (a) ordinate shift (b_p); (b) abscissa shift (a_p).

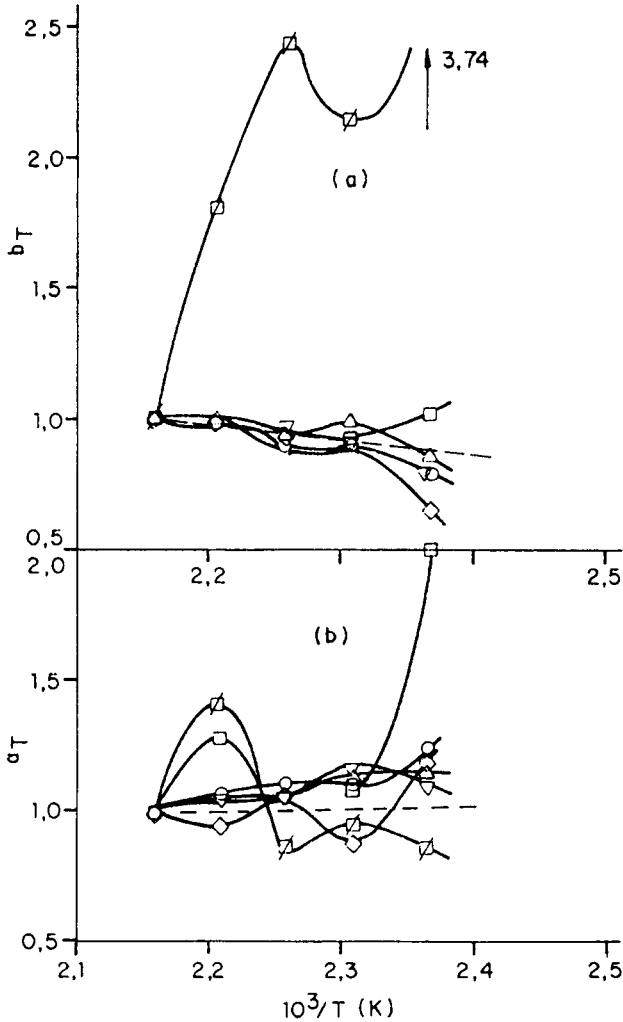


Figure 8 Temperature-shift factors (b_T and a_T) with reference temperature $T_0 = 463 \text{ K}$, at different pressures (\square) 5 MPa, (\diamond) 30 MPa, (\circ) 70 MPa, (Δ) 100 MPa, (∇) 130 MPa, (\square) 170 MPa: (a) ordinate shift (b_T); (b) abscissa shift [a_T , (----) computed with eq. (14)].

sidered¹³ as the compressibility (instantaneous¹²) of only the occupied volume, i.e., it corresponds to the absence of any intermolecular configurational rearrangements of the chain backbone within the time interval of the experiment. Their difference is the compressibility of the free volume alone.

The elastic energy storage recoverable after stress removal¹³ is

$$B_e = B_c^s - B_d^s \quad (15)$$

B_c^s and B_d^s are the steady-state creep compliances in the compression and decompression steps, respectively. B_e values are shown in Figure 10(a). It increases with increasing temperature and decreases

ing pressure. The ratio B_c^s/B_d^s is related [Fig. 10(b)] to the die-swell in extrusion (D/D_0),¹⁵ and increases with increasing stress (P) and temperature (T).

The bulk volume viscosity (η_K) is^{3,5}

$$\eta_K = \frac{-\Delta p}{\frac{\Delta V}{V_0} \cdot \frac{1}{\Delta t}} = \frac{\Delta t}{B_d^s} \quad (16)$$

Its values are shown in Figure 11 as a function of the compression stress. η_K increases with de-

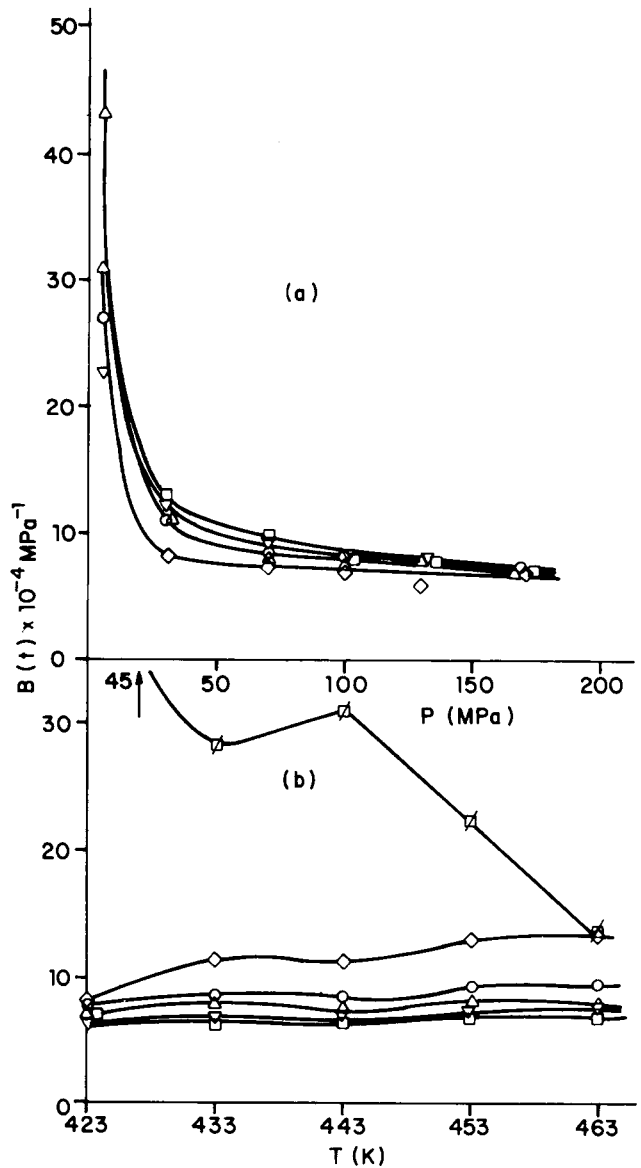


Figure 9 Bulk creep compliance $B(t)$ as a function of (a) pressure and different temperatures: (\diamond) 423 K, (\circ) 433 K, (Δ) 443 K, (∇) 453 K, (\square) 463 K; (b) temperature and different pressures (\square) 5 MPa, (\diamond) 30 MPa, (\circ) 70 MPa, (Δ) 100 MPa, (∇) 130 MPa, (\square) 170 MPa.

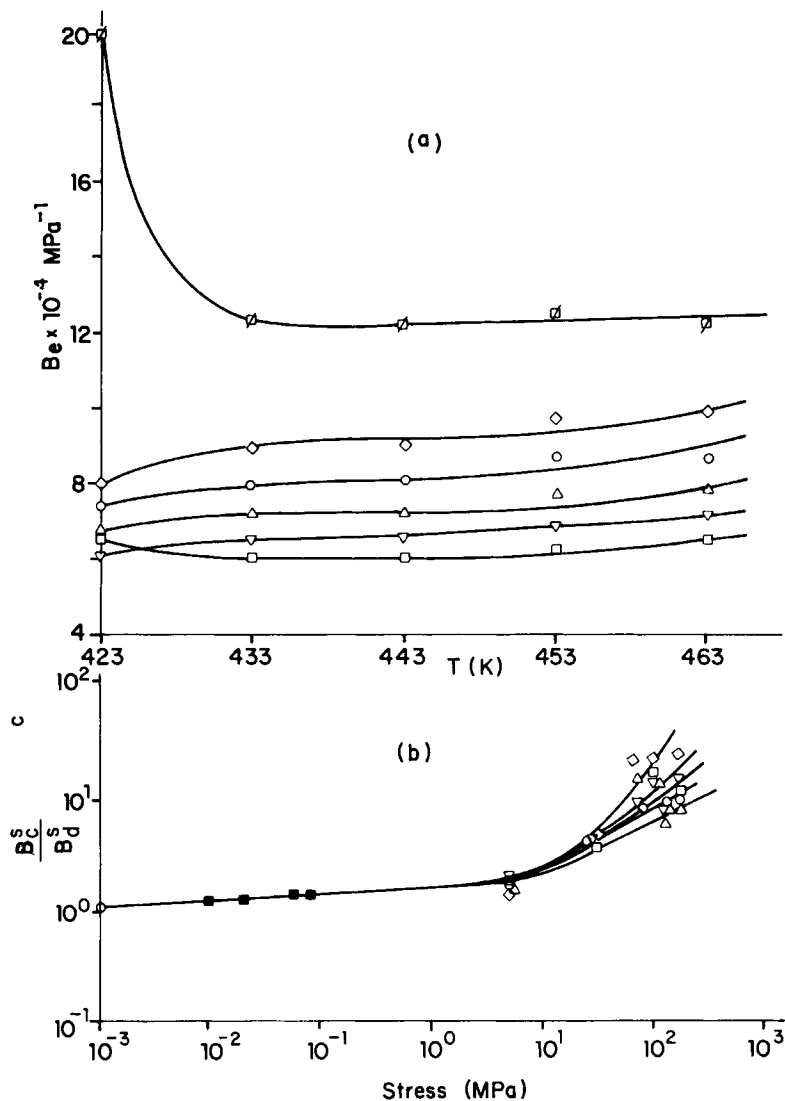


Figure 10 (a) LDPE steady-state bulk creep compliance (B_e) vs. temperature at (\square) 5 MPa, (\diamond) 30 MPa, (\circ) 70 MPa, (\triangle) 100 MPa, (∇) 130 MPa, (\square) 170 MPa; (b) LDPE die-swell vs. stress (P) in shear deformation at (\blacksquare) 463 K, (Ref. 11), and decompression at (\diamond) 423 K, (\circ) 433 K, (\triangle) 443 K, (∇) 453 K, (\square) 463 K.

creasing temperature³ and with decreasing pressure until about 50 MPa, and then remains almost constant (the differences observed being possibly provided by the variation of the compression rates around $0.5\text{--}2.0 \times 10^{-5} \text{ s}^{-1}$).

CONCLUSIONS

Compression creep of molten LDPE has been measured. LDPE flexible chains show volume deformations ($k\%$) that increase (contrary to rigid chain

polymers such as polystyrene [PS]⁵ in which $k\%$ decrease) as the temperature increases. Effect of temperature and pressure on bulk creep compliance $B(t)$ are described by shift factors, the ordinate ones (b_p , b_T) being governed by intramolecular interactions (ΔH), and the abscissa ones (a_T , a_p), by activation energy (ΔE) and activation volume (ΔV^*), respectively. LDPE bulk creep compliance $B(t)$ behavior is different below and above some critical value (T_c , P_c) of the process variables, at which a change of chain conformation from *gauche* to *trans* takes place. Bulk viscosity (η_K) data follow the pattern of the molecular motions just described.

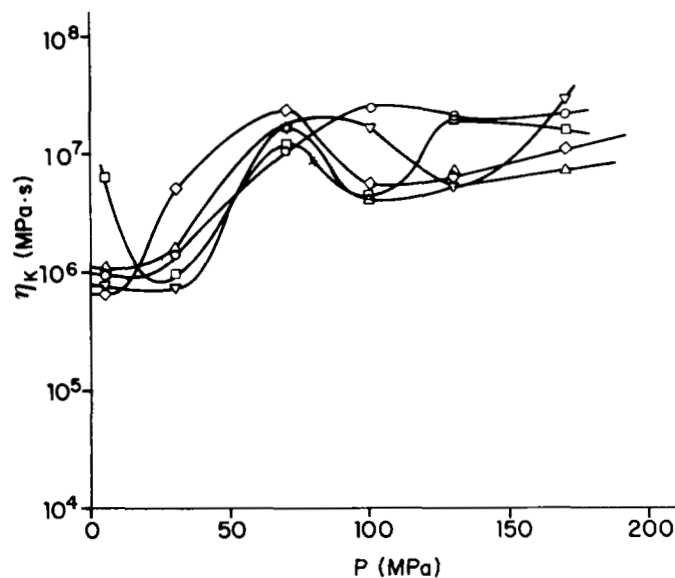


Figure 11 LDPE bulk viscosity (η_K) as a function of stress (P) at different temperatures: (\diamond) 423 K, (\circ) 433 K, (\triangle) 443 K, (∇) 453 K, (\square) 463 K.

REFERENCES

1. F. Hurtado-Laguna and J. V. Aleman, *J. Polym. Sci. Polym. Chem. Ed.*, **26**, 2631-2649 (1988).
2. J. V. Aleman (a) *Polymer*, to appear; (b) *Eur. Polym. J.*, **27**, 221-226 (1991).
3. J. V. Aleman, *Polym. Eng. Sci.*, **30**, 326-334 (1990).
4. J. V. Aleman, *Rheol. Acta*, **27**, 634-638 (1988).
5. J. V. Aleman, *Angew. Makromol. Chem.* **181**, 53-56 (1990).
6. S. Beret and J. M. Prausnitz, *Macromolecules*, **8**, 536-538 (1975).
7. S. Matsuoka, *J. Polym. Sci.*, **57**, 569-588 (1962).
8. K. H. Hellwege, W. Knappe, and P. Lehmann, *Kolloid Z. Z. Polym.* **183**, 110-120 (1961).
9. P. Zoller, *J. Appl. Polym. Sci.*, **23**, 1051-1056 (1979).
10. J. P. Lesbats, R. Legross, and J. V. Aleman, *J. Polym. Sci. Polym. Chem. Ed.*, **20**, 1971-1984 (1982).
11. L. Ming, G. G. Reind, and P. Zoller, *Polymer*, **29**, 1784-1788 (1988).
12. (a) A. J. Kovacs, *Trans. Soc. Rheol.*, **5**, 285-296 (1961); (b) J. J. Tribone, J. M. O'Reilly, and J. Greener, *J. Polym. Sci. Polym. Phys. Ed.*, **27**, 837-857 (1989).
13. J. D. Ferry, *Viscoelastic Properties of Polymers*, Wiley, New York, 1980.
14. T. Bleha and J. Gajdos, *Colloid Polym. Sci.*, **266**, 405-410 (1988).
15. E. B. Bagley, S. H. Storey, and D. C. West, *J. Appl. Polym. Sci.*, **7**, 1661-1672 (1963).

Received November 7, 1990.

Accepted April 24, 1991